can speculate that the RAMRIS synovitis score obtained with it is less accurate than the score obtained with the data of Haavardsholm et al. [18]. Also, differences in the therapies used (anti-TNF-α therapy versus initial synthetic DMARDs in the present study) and in the patient populations (established RA versus very early RA in the present study) may have led to the different results. In addition to anti-TNF-α therapy, the RAMRIS bone edema score has been shown to decrease with abatacept treatment for 6 months [19].

Considering that there is a high percentage of inflammatory cells in MRI-proven bone edema in RA patients [20], antirheumatic therapies are assumed to induce a dramatic change in bone edema. Since the observation period of this study (1 year) was short, and the number of patients (13) was small, further large cohort studies consisting of several therapeutic arms are needed to determine the real nature of bone edema in patients with RA.

Acknowledgments This study was supported in part by a grant from The Ministry of Health, Labour and Welfare, Japan.

Conflict of interest None.

References

1. Combe B, Landewe R, Lukas C, Bolosiu HD, Breedveld F, Dougados M, et al. EULAR recommendations for the management of early arthritis: report of a task force of the European Standing Committee for International Clinical Studies Including Therapeutics (ESCISIT). Ann Rheum Dis. 2007;66:34–45.
2. Smolen JS, Aletaha D, Bijlsma JW, Breedveld FC, Boumpas D, Burmester G, et al. Treating rheumatoid arthritis to target: recommendations of an international task force. Ann Rheum Dis. 2010;69:631–7.
3. Mease PJ. Improving the routine management of rheumatoid arthritis: the value of tight control. J Rheumatol. 2010;37:1570–8.
4. Aletaha D, Neogi T, Silman AJ, Funovits J, Felson DT, Bingham CO 3rd, et al. Rheumatoid arthritis classification criteria: an American College of Rheumatology/European League Against Rheumatism collaborative initiative. Arthr Rheum. 2010;62: 2569–81.
5. Aletaha D, Neogi T, Silman AJ, Funovits J, Felson DT, Bingham CO 3rd, et al. Rheumatoid arthritis classification criteria: an American College of Rheumatology/European League Against Rheumatism collaborative initiative. Ann Rheum Dis. 2010;69: 1580–8.
6. Tamai M, Kawakami K, Uetani M, Takao S, Arima K, Iwamoto N, et al. A prediction rule for disease outcome in patients with undifferentiated arthritis using magnetic resonance imaging of the wrist and finger joints and serologic autoantibodies. Arthr Rheum. 2009;61:772–8.
7. Hodgson RJ, O'Connor P, Moots R. MRI of rheumatoid arthritis—image quantitation for the assessment of disease activity, progression and response to therapy. Rheumatology. 2008;47: 13–21.
8. Østergaard M, Pedersen SJ, Døhn UM. Imaging in rheumatoid arthritis—status and recent advances for magnetic resonance imaging, ultrasonography, computed tomography and conventional radiography. Best Pract Res Clin Rheumatol. 2008;22: 1019–44.
9. Hetland M, Ejbjerg B, Horslev-Petersen K, Jacobsen S, Vestergaard A, Jurik AG, et al. MRI bone oedema is the strongest predictor of subsequent radiographic progression in early rheumatoid arthritis. Results from a 2-year randomised controlled trial (CIMESTRA). Ann Rheum Dis. 2009;68:384–90.
10. Hetland M, Stengaard-Pedersen K, Junker P, Østergaard M, Ejbjerg BJ, Jacobsen S, et al. Radiographic progression and remission rates in early rheumatoid arthritis—MRI bone oedema and anti-CCP predicted radiographic progression in the 5-year extension of the double-blind randomised CIMESTRA trial. Ann Rheum Dis. 2010;69:1789–95.
11. Kita J, Tamai M, Arima K, Nakashima Y, Suzuki T, Kawashiri S, et al. Treatment discontinuation in patients with very early rheumatoid arthritis in sustained simplified disease activity index remission after synthetic disease-modifying anti-rheumatic drug administration. Mod Rheumatol. 2011. doi:10.1007/s10165-011-0522-8
12. Arnett FC, Edworthy SM, Bloch DA, McShane DJ, Fries JF, Cooper NS, et al. The American Rheumatism Association 1987 revised criteria for the classification of rheumatoid arthritis. Arthr Rheum. 1988;31:315–24.
13. Tamai M, Kawakami A, Uetani M, Takao S, Tanaka F, Fujikawa K, et al. Bone edema determined by magnetic resonance imaging reflects severe disease status in patients with early-stage rheumatoid arthritis. J Rheumatol. 2007;34:2154–7.
14. Tamai M, Kawakami A, Iwamoto N, Kawashiri SY, Fujikawa K, Aramaki T, et al. Comparative study of the detection of joint injury in early-stage rheumatoid arthritis by MRI of wrist and finger joints and physical examination. Arthritis Care Res. 2011;63:436–9.
15. Aletaha D, Smolen JS. The Simplified Disease Activity Index (SDAI) and Clinical Disease Activity Index (CDAI) to monitor patients in standard clinical care. Best Pract Res Clin Rheumatol. 2007;21:663–75.
16. Sakai R, Komano Y, Tanaka M, Nanki T, Koike R, Nakajima A, et al. The REAL database reveals no significant risk of serious infection during treatment with a methotrexate dose of more than 8 mg/week in patients with rheumatoid arthritis. Mod Rheumatol. 2011;21:444–8.
17. Salaffi F, Carotti M, Ciapetti A, Gasparini S, Filippucci E, Grassi W. Relationship between time-integrated disease activity estimated by DAS28-CRP and radiographic progression of anatomical damage in patients with early rheumatoid arthritis. BMC Musculoskelet Disord. 2011;12:120.
18. Haavardsholm EA, Østergaard M, Hammer HB, Bøyesen P, Boonen A, van der Heijde D, et al. Monitoring anti-TNFα treatment in rheumatoid arthritis: responsiveness of magnetic resonance imaging and ultrasonography of the dominant wrist joint compared with conventional measures of disease activity and structural damage. Ann Rheum Dis. 2009;68:1572–9.
19. Emery P, Durez P, Dougados M, Legerton CW, Becker J-C, Vratsanos G, et al. Impact of T-cell costimulation modulation in patients with undifferentiated inflammatory arthritis or very early rheumatoid arthritis: a clinical and imaging study of abatacept (the ADJUST trial). Ann Rheum Dis. 2010;69:510–6.
20. Schett G. Bone marrow edema. Ann N Y Acad Sci. 2009;1154: 35–40.

Mod Rheumatol (2012) 22:654–658
DOI 10.1007/s10165-011-0575-8

ORIGINAL ARTICLE

Magnetic resonance imaging (MRI) detection of synovitis and bone lesions of the wrists and finger joints in early-stage rheumatoid arthritis: comparison of the accuracy of plain MRI-based findings and gadolinium-diethylenetriamine pentaacetic acid-enhanced MRI-based findings

Mami Tamai · Atsushi Kawakami · Masataka Uetani · Aya Fukushima · Kazuhiko Arima · Keita Fujikawa · Naoki Iwamoto · Toshiyuki Aramaki · Makoto Kamachi · Hideki Nakamura · Hiroaki Ida · Tomoki Origuchi · Kiyoshi Aoyagi · Katsumi Eguchi

Received: 25 July 2011 / Accepted: 25 November 2011 / Published online: 28 December 2011

Abstract
Objective To explore whether synovitis and bone lesions in the wrists and finger joints visualized by plain magnetic resonance imaging (MRI)-based findings correspond exactly or not to those judged by gadolinium-diethylenetriamine pentaacetic acid (Gd-DTPA)-enhanced MRI-based findings.

Methods Magnetic resonance imaging of the wrists and finger joints of both hands were examined in 51 early-stage rheumatoid arthritis (RA) patients whose median disease duration from the onset of articular manifestations to entry was 5 months, by both plain (T1 and short-time inversion recovery images) and Gd-DTPA-enhanced MRI (post-contrast fat-suppressed T1-weighted images) simultaneously. We focused on 15 sites per hand, to examine the presence of synovitis and bone lesions (bone edema and bone erosion). Gd-DTPA-enhanced MRI-based findings

M. Tamai and A. Kawakami contributed equally to this work.

M. Tamai (✉) · A. Kawakami · N. Iwamoto · M. Kamachi · H. Nakamura
Unit of Translational Medicine, Department of Immunology and Rheumatology, Graduate School of Biomedical Sciences, Nagasaki University, 1-7-1 Sakamoto, Nagasaki 852-8501, Japan
e-mail: tamaim@nagasaki-u.ac.jp

M. Tamai
Center for Health and Community Medicine, Nagasaki University, 1-14 Bunkyo-machi, Nagasaki 852-8521, Japan

M. Uetani · A. Fukushima
Department of Radiology and Radiation Research, Nagasaki University, 1-7-1 Sakamoto, Nagasaki 852-8501, Japan

K. Arima
Department of Medical Gene Technology, Atomic Bomb Disease Institute, Nagasaki University School of Health Sciences, Nagasaki University, 1-7-1 Sakamoto, Nagasaki 852-8501, Japan

K. Fujikawa
Department of Rheumatology, Isahaya Healthy Insurance General Hospital, 24-1 Eisyohigashi-machi, Isahaya 854-8501, Japan

T. Aramaki
Department of Rheumatology, Japanese Red Cross Nagasaki Genbaku Hospital, 3-15 Mori-machi, Nagasaki 852-8511, Japan

H. Ida
Division of Respirology, Neurology and Rheumatology, Department of Medicine, Kurume University, 67 Asahi-machi, Kurume 830-0011, Japan

T. Origuchi
Department of Rehabilitation Sciences, Nagasaki University, 1-7-1 Sakamoto, Nagasaki 852-8501, Japan

K. Aoyagi
Department of Public Health, Graduate School of Biomedical Sciences, Nagasaki University, 1-7-1 Sakamoto, Nagasaki 852-8501, Japan

K. Eguchi
Sasebo City General Hospital, 9-3 Hirase-machi, Sasebo 857-8511, Japan

were considered "true" lesions, and we evaluated the accuracy of plain MRI-based findings in comparison to Gd-DTPA-enhanced MRI-based findings.

Results Synovitis, judged by plain MRI-based findings, appeared as false-positive at pretty frequency; thus, the specificity, positive predictive value and accuracy of the findings were low. The rate of enhancement (E-rate) in false-positive synovitis sites was significantly low compared with true-positive synovitis sites where Gd-DTPA enhancement appears. In contrast to synovitis, the false-positivity of bone lesions, judged by plain MRI-based findings, was very low compared with Gd-DTPA-enhanced MRI-based findings.

Conclusion Synovitis judged by plain MRI-based findings is sometimes considered false-positive especially in sites where synovitis is mild. However, plain MRI is effective in identifying bone lesions in the wrist and finger joints in early-stage RA.

Keywords Early-stage RA · Plain MRI · Gd-DTPA-enhanced MRI · Synovitis · Bone lesions

Abbreviations

ACR	American College of Rheumatology
CRP	C-reactive protein
E-rate	Rate of enhancement
Gd-DTPA	Gadolinium–diethylenetriamine pentaacetic acid
HLA-DRB1*SE	HLA-DRB1*shared epitope
RA	Rheumatoid arthritis
UA	Undifferentiated arthritis

Introduction

Magnetic resonance imaging (MRI) reveals joint inflammation and damage in early-stage rheumatoid arthritis (RA) [1–4] that take the form of synovitis and bone lesions, including bone edema and bone erosion [1–4]. As active synovial lesions in patients with RA are rich in vascularity, gadolinium-diethylenetriamine pentaacetic acid (Gd-DTPA)-enhanced MRI-based findings have become the gold standard to evaluate joint inflammation and damage in RA [1]. Accordingly, by assessing Gd-DTPA-enhanced MRI-based findings of the wrists and finger joints of both hands, we have determined that symmetrical synovitis and bone lesions are important predictors of the development of RA in patients with undifferentiated arthritis (UA) [5–8]. In these earlier studies, we did not specifically compare Gd-DTPA-enhanced MRI-based findings with plain MRI-based findings. However, Gd-DTPA-enhanced MRI is an expensive diagnostic tool compared to plain MRI, and Gd-DTPA can induce serious adverse events [9]. Thus, if plain MRI is sufficiently sensitive for the purpose, it should be possible to reduce both the cost and the adverse events associated with Gd-DTPA by using plain MRI.

The aim of the study reported here was to determine whether plain MRI-based findings are effective in evaluating joint inflammation and damage in early-stage RA in comparison to Gd-DTPA-enhanced MRI-based findings. Our results suggest that plain MRI is a sufficiently sensitive diagnostic tool to evaluate bone lesions, but that synovitis determined by plain MRI-based findings may on occasion appear as a false-positive, especially at sites where synovitis is mild.

Patients and methods

Patients

The Early Arthritis Clinic opened in 2001 as part of the Unit of Translational Medicine of the Department of Immunology and Rheumatology of the Graduate School of Biomedical Sciences of Nagasaki University. It is a regional center for the treatment of arthritis, with patients from the whole western part of Japan, Nagasaki Prefecture (approx. 450,000 inhabitants) being referred there for treatment. For our study, we recruited 51 early-stage RA patients from this clinic. The disease status of these patients was formally confirmed by a rheumatologist in our department, and a diagnosis of RA was based on the 1987 criteria for RA of the American College of Rheumatology (ACR) [10]. Baseline clinical manifestations and variables included sex, age, localization of arthritis, morning stiffness, number of tender joints, number of swollen joints, C-reactive protein level (CRP; measured by latex turbidimetric immunosorbent assay; Daiichi Pure Chemicals, Fukuoka, Japan), immunoglobulin M-rheumatoid factor (IgM-RF) positivity (measured by latex-enhanced immunonephelometric assay; cut-off value 14 IU/ml; Dade Behring, Marburg, Germany), positive status for anti-cyclic citrullinated peptide (CCP) antibodies (measured by enzyme-linked immunosorbent assay; cut-off value 4.5 U/ml; DIASTAT Anti-CCP; Axis-Shield, Dundee, UK), HLA-DRB1 genotyping, and MRI findings for both the wrists and finger joints, as previously described [5–8, 11]. All variables were examined on the same day, as previously reported [5–8, 11]. Each patient provided a signed consent form to participate in the study, which was approved by the Institutional Review Board of Nagasaki University.

MRI of wrists and finger joints

Magnetic resonance scan images of both the wrists and finger joints were acquired using a 1.5 T system (Signa; GE Medical Systems, Milwaukee, WI) with an extremity coil. T1-weighted spin-echo (TR 450 ms, TE 13 ms) images, short-time inversion recovery (STIR; TR 3000 ms, TE 12 ms, T1 160 ms) images, and Gd-DTPA-enhanced images were simultaneously acquired. The images were evaluated for bone edema, bone erosion, and synovitis in 15 sites in each finger and wrist: the distal radioulnar joint, the radiocarpal joint, the midcarpal joint, the first carpometacarpal joint, the second-fifth carpometacarpal joints (together), the first–fifth metacarpophalangeal joints, and the first–fifth proximal interphalangeal joints (PIP joints) separately (a total of 30 sites in both hands), as recently reported [5–8, 11]. The presence of synovitis, bone edema, and bone erosion was evaluated according to the methods described by Lassere et al. [12] and Conaghan et al. [13], by two experienced radiologists (M.U. and A.F.), and decisions were reached by consensus, as previously described [5–8, 11]. Since the focus of our study was to compare MRI-based findings and Gd-DTPA-enhanced MRI-based findings in terms of their accuracy in determining synovitis and bone change, we included bone edema and bone erosion as bone lesions in our study. Gd-DTPA-enhanced images were obtained by intravenous injection of 0.1 mmol/kg of Gd-DTPA (Magnevist; Bayer Schering Pharma, Berlin, Germany). A dynamic study was performed to evaluate the vascularity of the affected joints as a rate of enhancement (E-rate), which was determined by examining coronal sections taken at 4-s intervals over a 150-s time period with fast spoiled gradient recalled acquisition in the steady state (SPGR) sequences, as previously described [5–8, 11].

Comparison of plain MRI-based findings and Gd-DTPA-enhanced MRI-based findings

Gd-DTPA-enhanced MRI-based findings are the gold standard for evaluating joint inflammation and damage by MRI in RA [1]. Thus, we assumed that Gd-DTPA-enhanced MRI-based findings represented "true" lesions and subsequently calculated the accuracy of plain MRI-based findings, comparing sensitivity, specificity, positive predictive value (PPV), negative predictive value (NPV), and accuracy.

Statistical analysis

Differences between the groups shown in Table 4 were examined for statistical significance using the Mann–Whitney U test. A P value of <0.05 was taken to indicate a statistically significant difference.

Results

Patient characteristics

Table 1 shows the baseline characteristics of the 51 patients with RA enrolled in our study. Since the median disease duration from the onset of articular manifestations to entry was 5 months, this study population was considered to have early-stage RA. The median Genant-modified Sharp score of the 51 patients at baseline was 0.49, which also identifies them as early-stage RA patients. The rates of seropositivity of IgM-RF and anti-CCP antibodies were 62.7 and 74.5%, respectively, and the rates of carriership of the HLA-DRB1*0405 allele and HLA-DRB1*shared epitope (SE) allele were 44.0 and 56.0%. These characteristics of autoantibodies and HLA-DR typing indicate that our study population manifested typical RA characteristics.

Synovitis and bone lesions of the wrists and finger joints of both hands according to plain MRI-based findings and Gd-DTPA-enhanced MRI-based findings

Among the 1530 sites of interest, we were able to evaluate synovitis in 1416 sites on both plain MR and Gd-DTPA-enhanced MR scan images. Synovitis was considered positive in 65.6% of sites (929/1416) according to plain MRI-based findings, but was not found in 316 of these 929 sites by Gd-DTPA-enhanced MRI-based findings

Table 1 Demographic features of 51 early-stage rheumatoid arthritis patients

Demographic feature	Value
Gender (M:F, % F)	8:43 (84.3%)
Age (years)	52 (19–80)
Duration (months)	5 (1–28)
Distribution of arthritis	
Symmetric (%)	82.4
Only upper extremities (%)	27.5
Both upper and lower extremities (%)	72.5
Genant-modified Sharp score	0.49 (0–8.58)
Positivity of IgM-RF (%)	62.7
IgM-RF (IU/ml)	18.0 (4.5–395)
Positivity of anti-CCP antibodies (%)	74.5
Anti-CCP antibodies (IU/ml)	24.3 (0.6–2115.3)
Positivity of CRP (%)	70.0
CRP (mg/dl)	1.14 (0.03–11.13)
Carriership of HLA-DRB1*0405 (%)	44.0 (diploid: 8.0%)
Carriership of HLA-DRB1*shared epitope (%)	56.0 (diploid: 8.0%)

Values are given as the median with the range in parenthesis, unless otherwise stated

M Male, *F* female, *IgM* immunoglobulin M, *RF* rheumatoid factor, *CCP* cyclic citrullinated peptide, *CPR* C-reactive protein

Table 2 Comparison of plain MRI-based findings to Gd-DPTA-enhanced MRI-based findings

MRI findings	Gd-enhanced MRI		Total
	Synovitis (+)	Synovitis (−)	
Synovitis			
Plain MRI			
Synovitis (+)	613	316	929
Synovitis (−)	175	312	487
Total	788	628	1416
Bone lesions			
Plain MRI			
Bone lesions (+)	92	9	101
Bone lesions (−)	22	1378	1400
Total	114	1387	1501

Synovitis were evaluated in 1416 sites and bone lesions were evaluated in 1501sites as described in Patients and methods

Gd-DPTA Gadolinium–diethylenetriamine pentaacetic acid, *MRI* magnetic resonance imaging

Table 3 Sensitivity, specificity, PPV, NPV and accuracy of synovitis and bone lesions according to the plain MRI-based findings[a]

	Sensitivity (%)	Specificity (%)	PPV (%)	NPV (%)	Accuracy (%)
Synovitis	77.8	49.7	66.0	64.1	65.3
Bone lesions	80.7	99.4	91.1	98.4	97.9

PPV Positive predictive value, *NPV* negative predictive value

[a] Gd-DTPA enhanced MRI-based findings were considered as gold standard; the accuracy of plain MRI-based findings were compared with Gd-DTPA-enhanced MRI-based findings

(Table 2). These data indicate that some synovitis that appears positive on a plain MR image scan is, in fact, false-positive. Bone lesions were visualized in 1501 sites by both plain and Gd-DTPA-enhanced MRI. In contrast to synovitis, the false-positive rate of bone lesions based on plain MRI findings was very low compared with that based on Gd-DTPA-enhanced MRI findings (Table 2). The rates of sensitivity, specificity, PPV and negative predictive value (NPV), and the accuracy of synovitis and bone lesion readings according to plain MRI were determined (Table 3).

The E-rate in sites of false-positive synovitis was significantly low compared with that in sites of true-positive synovitis

For the purposes of our study, the sites where plain MR scan images were positive for synovitis and Gd-DTPA-enhanced MR scan images were negative were considered to be false-positive sites; the sites for which positive results were obtained using both MRI imaging techniques were considered to be true positive sites. The severity of synovitis was compared by the E-rate of Gd-DTPA-enhanced MRI. As shown in Table 4, the E-rate of false-positive synovitis sites was significantly low compared with that of the true positive sites.

Table 4 Comparison of E-rate in sites of false-positive synovitis with sites of true-positive synovitis

MRI findings	N (sites)	E-rate (mean ± sd, median, range)	*P*-value
A. True positive; plain (+), enhanced (+)	366	8.1±5.1 (6.9, 1.2 – 50.1)	
B. False negative; plain (-), enhanced (+)	57	6.8 ±2.2 (6.5, 3.4 – 14.6)	N.S.
C. False positive; plain (+), enhanced (-)	121	5.7±2.2 (6.0, 1.4 – 14.5)	§
D. True negative; plain (-), enhanced (-)	298	5.5±1.7 (5.5, 1.4 – 12.3)	N.S.
			§
			§
			§

We compared every E-rate by Mann–Whitney *U* test. *P* values are as follows: A vs B, 0.19; A vs C, 9.2×10^{-10}; A vs D, 5.2×10^{-8}; B vs C, 0.00096; B vs D, 5.3×10^{-6} and C vs D, 0.20. It is interesting to note that E-rate of false-negative synovitis sites tended to be low, however, there is no statistical significance as compared with true-positive sites (see A vs B). E-rate of false-negative synovitis sites was high as compared with false-positive synovitis sites (see B vs C)

§ *P* value <0.0001

Discussion

Recent reviews have reported that plain MRI-based findings of bone lesions can be substituted for Gd-DTPA-enhanced MRI-based findings, although Gd-DTPA enhancement is recommended for the evaluation of synovitis [1]. Since the median disease duration from the onset of articular manifestations to entry in the 51 patients of our study cohort was 5 months, we suggest that our data reflect primarily rheumatoid joint damage, rather than secondary changes due to osteoarthritis. However, there have been few precise comparisons of plain MRI-based findings and Gd-DTPA-enhanced MRI-based findings; i.e., both plain and Gd-DTPA-enhanced sequences of multiple sites in both hands examined simultaneously. Ostergaard et al. reported that Gd-DTPA injection is not important to qualify the MRI scores of bone erosion and bone edema, whereas it is indispensable to diagnose synovitis [14].

Our data also show that plain MRI-based findings are not sufficient alone to evaluate the presence of synovitis. The severity of synovitis, as determined by the E-rate in dynamic Gd-DTPA-enhanced MR scan images, is low in false-positive synovitis sites compared with true-positive

sites. We speculate that cartilage, synovial fluids, or fibrous tissues may be interpreted as synovial hyperplasia in these cases, and we must be aware of the superiority of Gd-DTPA-enhanced MRI over plain MRI in evaluating synovitis, especially in the case of less active lesions. The E-rate of false-negative synovitis sites tended to be low among our patients; however, there was no statistical significance relative to true-positive synovitis sites. Accordingly, the E-rate of false-negative synovitis sites was high as compared with that of false-positive synovitis sites. Since a previous study demonstrated that the E-rate of the wrist correlates with the clinical disease activity in patients with RA [15], we suggest that the E-rate could correlate well with the synovitis score based on the RA MRI scoring system (RAMRIS). Consequently, findings from Gd-DTPA-enhanced MRI are crucial to qualify the presence of synovitis correctly.

Nevertheless, plain MRI is an effective tool for evaluating bone lesions of the wrists and finger joints since false-positivity is very low for this evaluation. In addition to the wrists and metacarpophalangeal joints, we identified three PIP joints as being positively associated with bone lesions out of 114 sites which were identified by Gd-enhanced MRI. There was no false-positive result by plain MRI in these three PIP joints, indicating that plain MRI is able to accurately detect the bone lesions of smaller joints of PIP joints. A recent observation (unpublished data) by our group indicates that the E-rate of sites with bone lesions is significantly high compared with that of those without bone lesions [15]. These data suggest that synovial inflammation is obvious in bone lesion sites and, therefore, that false-positivity is low in these areas.

In summary, our present data confirm the recent results of Ostergaard et al. [14] that bone lesions can be correctly identified by plain MRI-based findings in early-stage RA, while synovitis cannot. Based on our present results, we are currently investigating longitudinal changes in bone lesions by plain MRI of the wrists and finger joints in early arthritis patients during therapeutic interventions. These studies are warranted to establish the value of plain MRI in clinical rheumatology.

Acknowledgments This study was supported in part by a Grant from The Ministry of Health, Labour and Welfare, Japan.

Conflict of interest None.

References

1. Østergaard M, Pedersen SJ, Døhn UM. Imaging in rheumatoid arthritis: status and recent advances for magnetic resonance imaging, ultrasonography, computed tomography and conventional radiography. Best Pract Res Clin Rheumatol. 2008;22:1019–44.
2. Kubassova O, Boesen M, Peloschek P et al. Quantifying disease activity and damage by imaging in rheumatoid arthritis and osteoarthritis. Ann N Y Acad Sci. 2009;1154:207–38.
3. McQueen FM. The use of MRI in early RA. Rheumatology (Oxf). 2008;47:1597–9.
4. McGonagle D, Tan AL. What magnetic resonance imaging has told us about the pathogenesis of rheumatoid arthritis: the first 50 years. Arthritis Res Ther. 2008;10:222.
5. Tamai M, Kawakami A, Uetani M et al. A prediction rule for disease outcome in patients with undifferentiated arthritis using MRI of wrists and finger joints and serologic autoantibodies. Arthritis Rheum. 2009;61:772–8.
6. Tamai M, Kawakami A, Uetani M et al. Bone edema determined by magnetic resonance imaging reflects severe disease status in patients with early-stage rheumatoid arthritis. J Rheumatol. 2007;34:2154–7.
7. Tamai M, Kawakami A, Uetani M et al. Early prediction of rheumatoid arthritis by serological variables and magnetic resonance imaging of the wrists and finger joints: results from prospective clinical examination. Ann Rheum Dis. 2006;65:134–5.
8. Tamai M, Kawakami A, Uetani M et al. The presence of anti-cyclic citrullinated peptide antibody is associated with magnetic resonance imaging detection of bone marrow oedema in early stage rheumatoid arthritis. Ann Rheum Dis. 2006;65:133–4.
9. Ersoy H, Rybicki FJ. Biochemical safety profiles of gadolinium-based extracellular contrast agents and nephrogenic systemic fibrosis. J Magn Reson Imaging. 2007;26:1190–7.
10. Arnett FC, Edworthy SM, Bloch DA et al. The American Rheumatism Association 1987 revised criteria for the classification of rheumatoid arthritis. Arthritis Rheum. 1988;31:315–24.
11. Fujikawa K, Kawakami A, Tamai M et al. High serum cartilage oligomeric matrix protein determines the subset of patients with early-stage rheumatoid arthritis with high serum C-reactive protein, matrix metalloproteinase-3 and MRI-proven bone erosion. J Rheumatol. 2009;36:1126–9.
12. Lassere M, McQueen F, Østergaard M et al. OMERACT Rheumatoid arthritis magnetic resonance imaging studies. Exercise 3: an international multicenter reliability study using the RA-MRI Score. J Rheumatol. 2003;30:1366–75.
13. Conaghan P, Lassere M, Østergaard M, Peterfy C, McQueen F, O'Connor P et al. OMERACT Rheumatoid Arthritis Magnetic Resonance Imaging Studies. Exercise 4: an international multicenter longitudinal study using the RA-MRI Score. J Rheumatol. 2003;30(6):1376–9.
14. Ostergaard M, Conaghan PG, O'Connor P, Szdudlarek M, Klarlund M, Emery P, et al. Reducing invasiveness, duration, and cost of magnetic resonance imaging in rheumatoid arthritis by omitting intravenous contrast injection—does it change the assessment of inflammatory and destructive joint changes by the OMERACT RAMRIS? J Rheumatol. 2009;36:1806–10. (Erratum in: J Rheumatol. 2010;27:2198).
15. Cimmino MA, Innocenti S, Livrone F, Magnaguagno F, Silvestri E, Garlaschi G. Dynamic gadolinium-enhanced magnetic resonance imaging of the wrist in patients with rheumatoid arthritis can discriminate active from in active disease. Arthritis Rheum. 2003;48(5):1207–13.

Contrast-enhanced whole body joint MR Imaging in rheumatoid patients on tumour necrosis factor-alpha agents: a pilot study to evaluate novel scoring system for MR synovitis

Sirs,

In the past decade the development of biological agents particularly those which target tumour necrosis factor alpha (anti-TNF-α) has started a new era in the management of rheumatoid arthritis (RA). Data from recent studies in patients with RA show that these drugs are very effective in improving clinical and functional outcomes, and have demonstrated the ability to arrest or even reverse radiographic progression (1, 2). In recent years, magnetic resonance imaging (MRI) has increasingly been used as outcome measures in clinical trials of RA (3, 4). Presence of inflammatory involvement of joints other than the hand especially if clinically occult, potentially alter treatment. The aims of the present study were to introduce and describe a novel scoring system for the assessment of whole body joint synovitis, and to assess the relationship with clinical findings in a longitudinal setting in rheumatoid patients treated with anti-TNF-α agents.

The study, which met the requirements of our institutional review board for a retrospective observational study, included 12 consecutive patients (2 men and 10 women; median age, 60 years; age range, 35–73 years) who started anti-TNF-α treatment. The patients had arthritis with a median symptom duration of 55 months (range: 7–276 months), receiving various dose of methotrexate. All patients satisfied the American College of Rheumatology revised 1987 criteria for RA (5) at the time of entry.

Ten patients received intravenous injections of infliximab (Remicade; Tanabe Pharmaceutical, Tokyo, Japan) and 4 patients received etanercept (Enbrel; Amgen, Pfizer/Wyeth, Takeda). The kinds and amounts of other drugs that each patient was taking were not changed during the study period. Each patient was clinically evaluated and underwent MR imaging at baseline and followup. Contrast enhanced MRI was performed on a 1.5T whole body MR system (Magnetom Avanto; Siemens Medical Solutions, Erlangen, Germany) in a way described elsewhere (6). Briefly, the joints of 13 body regions for each patient: the atlanto-axial joint, bilateral shoulder joints, bilateral wrist joints, bilateral MCP joints, bilateral hip joints, bilateral knee joints, and bilateral metatarsophalangeal (MTP) joints were scanned and evaluated. Image acquisition was started immediately after completing contrast injection and joints were scanned in the order mentioned above. The examination time was less than 30 minutes. The MR images were assessed by one experienced radiologist, who was blinded to all clinical information. Hand joints were evaluated according to RAMRIS for synovitis. Remaining joints were scored in the similar way as RAMRIS for hand joints (7).

Table. Correlation in treatment effect between MR measures and clinical data / disease activity.

	ΔMR-positive joint count			ΔMR synovitis score		
	Total	Hand	Remaining	Total	Hand	Remaining
ΔTJC	0.573*	NS	0.554*	0.620*	NS	0.642*
ΔSJC	NS	NS	0.587*	0.598*	NS	0.647*
ΔVAS	NS	NS	NS	NS	NS	NS
ΔESR (mm/hr)	NS	NS	NS	NS	NS	NS
ΔCRP (mg/dl)	NS	NS	NS	NS	NS	NS
ΔDAS28-ESR	NS	NS	NS	0.576*	NS	NS

Δ (delta) means difference between baseline and follow-up studies. *$p<0.05$.

Both MR-positive joint count and MR synovitis score for hands joints did not correlate with any of the measures for clinical data and disease activity. On the other hand, both MR-positive joint count and MR synovitis score for remaining joints correlated moderately to strongly with some measures for clinical data and disease activity. There was moderate positive correlation between delta MR synovitis score for total joints (hands and remaining joints) and delta DAS28-ESR. Here, delta means the difference between baseline and follow-up studies (Table I).

MR imaging findings of the systemic joints correlate with clinical findings in RA patients, especially when scoring analysis for synovitis is performed. Compared to hand joints, changes in MR synovitis score caused by therapeutic agent such as anti-TNF-α may be more sensitive in remaining joints. This may indicate that images obtained beyond the appropriate time window of 5–10 minutes after contrast injection (8) are useful to evaluate the response to treatment. Although the group of patients studied was small and non homogeneus, this approach may be useful for sensitive analysis of systemic synovitis in rheumatoid patients. Study with a greater number of patients with healthy controls is necessary to obtain more solid conclusions.

T. KAMISHIMA[1], *MD, PhD*
M. KATO[2], *MD, PhD*
T. ATSUMI[3], *MD, PhD*
T. KOIKE[4], *MD, PhD*
Y. ONODERA[5], *MD, PhD*
S. TERAE[5], *MD, PhD*

[1]Faculty of Health Science, Hokkaido University Sapporo, Japan; [2]Center of Experimental Rheumatology, University Hospital of Zurich, Zurich, Switzerland; [3]Department of Internal Medicine II, Hokkaido University Hospital, Sapporo, Japan; [4]NTT East Sapporo Hospital, Sapporo, Japan; [5]Department of Diagnostic Radiology, Hokkaido University Hospital, Sapporo, Japan.

Address correspondence to: Dr T. Kamishima, Faculty of Health Science, Hokkaido University Hospital, N15 W7, Kita-Ku, Sapporo City, 0600815 Japan.
E-mail: ktamotamo2@yahoo.co.jp

Competing interests: none declared.

References

1. KLARESKOG L, VAN DER HEIJDE D, DE JAGER JP *et al.*: Therapeutic effect of the combination of etanercept and methotrexate compared with each treatment alone in patients with rheumatoid arthritis: double-blind randomised controlled trial. *Lancet* 2004; 363: 675-81.
2. LIPSKY PE, VAN DER HEIJDE DM, ST CLAIR EW *et al.*: Infliximab and methotrexate in the treatment of rheumatoid arthritis. Anti-Tumor Necrosis Factor Trial in Rheumatoid Arthritis with Concomitant Therapy Study Group. *N Engl J Med* 2000; 343: 1594-602.
3. QUINN MA, CONAGHAN PG, O'CONNOR PJ *et al.*: Very early treatment with infliximab in addition to methotrexate in early, poor-prognosis rheumatoid arthritis reduces magnetic resonance imaging evidence of synovitis and damage, with sustained benefit after infliximab withdrawal: results from a twelve-month randomized, double-blind, placebo-controlled trial. *Arthritis Rheum* 2005; 52: 27-35.
4. OSTERGAARD M, DUER A, NIELSEN H *et al.*: Magnetic resonance imaging for accelerated assessment of drug effect and prediction of subsequent radiographic progression in rheumatoid arthritis: a study of patients receiving combined anakinra and methotrexate treatment. *Ann Rheum Dis* 2005; 64: 1503-6.
5. ARNETT FC, EDWORTHY SM, BLOCH DA *et al.*: The American Rheumatism Association 1987 revised criteria for the classification of rheumatoid arthritis. *Arthritis Rheum* 1988; 31: 315-24.
6. KAMISHIMA T, FUJIEDA Y, ATSUMI T *et al.*: Contrast-enhanced whole-body joint MRI in patients with unclassified arthritis who develop early rheumatoid arthritis within 2 years: feasibility study and correlation with MRI findings of the hands. *AJR Am J Roentgenol* 2010; 195: W287-92.
7. TAKASE K, OHNO S, TAKENO M *et al.*: Simultaneous evaluation of long-lasting knee synovitis in patients undergoing arthroplasty by power Doppler ultrasonography and contrast-enhanced MRI in comparison with histopathology. *Clin Exp Rheumatol* 2012; 30: 85-92.
8. YAMATO M, TAMAI K, YAMAGUCHI T, OHNO W: MRI of the knee in rheumatoid arthritis: Gd-DTPA perfusion dynamics. *J Comput Assist Tomogr* 1993; 17: 781-5.

RHEUMATOLOGY

Rheumatology 2013;52:523–528
doi:10.1093/rheumatology/kes310
Advance Access publication 28 November 2012

Concise report

Positive synovial vascularity in patients with low disease activity indicates smouldering inflammation leading to joint damage in rheumatoid arthritis: time-integrated joint inflammation estimated by synovial vascularity in each finger joint

Jun Fukae[1], Masato Isobe[1], Akemi Kitano[1], Mihoko Henmi[1], Fumihiko Sakamoto[1], Akihiro Narita[1], Takeya Ito[1], Akio Mitsuzaki[1], Masato Shimizu[1], Kazuhide Tanimura[1], Megumi Matsuhashi[1], Tamotsu Kamishima[2], Tatsuya Atsumi[3] and Takao Koike[3]

Abstract

Objective. To investigate the relationship between synovial vascularity and joint damage progression in each finger joint of patients with RA under low disease activity during treatment with biologic agents.

Methods. We studied 310 MCP and 310 PIP joints of 31 patients with active RA who were administered adalimumab (ADA) or tocilizumab (TCZ). Patients were examined with clinical and laboratory assessments. Power Doppler sonography was performed at baseline and at weeks 8, 20 and 40. Synovial vascularity was evaluated according to quantitative measurement. Hand and foot radiography was performed at baseline and at week 50.

Results. Composite scores of the DAS with 28 joints and the Simplified Disease Activity Index (SDAI) were significantly decreased from baseline to week 8, being sustained at a low level by biologic agents during the observational period. MCP and PIP joints with positive synovial vascularity after week 8 showed more subsequent joint damage progression than joints without synovial vascularity throughout the follow-up. The changes in radiographic progression in these joints were independent of the sum of synovial vascularity from baseline to week 40 or the occasional occurrence of positive synovial vascularity.

Conclusion. Smouldering inflammation reflected by positive synovial vascularity under low disease activity was linked to joint damage. The damage progressed irrespective of the severity of positive synovial vascularity. Even with a favourable overall therapeutic response, monitoring of synovial vascularity has the potential to provide useful joint information to tailor treatment strategies.

Trial registration. University Hospital Medical Information Network Clinical Trials Registry; http://www.umin.ac.jp/ctr/; UMIN000004476.

Key words: rheumatoid arthritis, power Doppler sonography, synovial vascularity, low disease activity.

[1]Hokkaido Medical Center for Rheumatic Diseases, [2]Faculty of Health Science, Hokkaido University Graduate School of Health Science and, [3]Department of Medicine II, Hokkaido University Graduate School of Medicine, Sapporo, Japan.

Submitted 31 July 2012; revised version accepted 27 September 2012.

Correspondence to: Jun Fukae, Hokkaido Medical Center for Rheumatic Diseases, 1-45, 3-Chome, 1-Jo, Kotoni, Nishi-ku, Sapporo 063-0811, Japan. E-mail: jun.fukae@ryumachi-jp.com

Introduction

In RA, clinical evaluations for disease activity such as patients' symptoms, joint examinations and laboratory data do not have enough power to provide details on local joint inflammation [1]. To assess rheumatoid disease activity, composite scores such as the ACR core data set or the DAS with 28 joints (DAS28) have been developed to

compensate for the weak points in the use of a single clinical marker [2, 3]. Although these composite scores have been well established as disease activity markers, they cannot precisely predict the destruction of individual joints.

The appearance and increase in synovial vascularity related to vasodilation and angiogenesis indicates active joint inflammation [4]. Power Doppler sonography (PDS) enables visualization of synovial vascularity and numerical representation of local inflammation [5, 6].

We focused on the clinical significance of synovial vascularity in RA. We previously reported the prediction of the progression of local finger joint damage via early changes in synovial vascularity [7, 8]. Interestingly, we observed finger joints with persistence of synovial vascularity after achieving low disease activity. Here we report on the relationship between synovial vascularity and joint damage progression in two patient groups treated with different biologic agents, focusing on finger joints with positive synovial vascularity after achieving low disease activity.

Patients and methods

Patients

Thirty-one patients with RA who had started adalimumab (ADA) or tocilizumab (TCZ) therapies were analysed. The patients had been pre-treated with DMARDs [ADA: eight patients with MTX, one with tacrolimus (TAC), one with bucillamine (BUC) + TAC, one with MTX + TAC and one with SSZ + TAC; TCZ: nine patients with MTX, one with BUC and two with TAC] or pre-treated with biologic agents [ADA: one patient with MTX + infliximab (IFX); TCZ: three patients with MTX + IFX, one with MTX + etanercept and two with MTX + ADA]. Despite these treatment histories, all patients were refractory cases having at least one swollen joint in the MCP/PIP joints and a DAS28-ESR > 3.2. Demographic, clinical and laboratory characteristics of the patients are shown in Table 1. After baseline examinations, ADA was given to 13 patients and TCZ to 18 patients. The biologic agents were given according to the standard protocols (ADA 40 mg s.c. injection bi-weekly, TCZ 8 mg/kg i.v. infusion every 4 weeks). This study was conducted in accordance with the Declaration of Helsinki and was approved by the local ethics committee of Hokkaido Medical Center for Rheumatic Diseases. Informed consent was obtained from all patients before they entered the study.

Clinical examination

Swollen and tender joints and global assessment on a visual analogue scale (VAS) were assessed at baseline and at weeks 8, 20 and 40 by rheumatologists (J.F., M.S., M.M., K.T.) who were blinded to the ultrasonographic results. Blood tests for ESR and CRP were performed at each assessment.

Ultrasonography and assessment

Ultrasonography was performed at baseline and at weeks 8, 20 and 40 by one of three US experts (M.H., F.S., A.N.) specialized in musculoskeletal ultrasonography who were blinded to other clinical information. A linear array transducer (13 MHz) and ultrasonographic machine were used (EUP-L34P, EUB-7500, Hitachi, Tokyo, Japan). Power Doppler settings have been previously described [7, 8]. First to fifth MCP and first to fifth PIP joints were scanned in the longitudinal plane over the dorsal surface. The quantitative PDS method was established in a previous report [8]. A value of synovial vascularity was determined by counting the number of vascular flow pixels in the region of interest.

Radiography and assessment

Plain radiographs of hands, wrists and feet were obtained at baseline and at week 50. Radiological assessments were examined according to the Genant-modified Sharp score (GSS) by a rheumatologist (M.S.) who was blinded to other clinical information [9].

Statistical analysis

Differences of composite parameters were examined using the Student's *t*-test and other data were examined using a non-parametric test (Wilcoxon's signed-rank test and Mann–Whitney U test). Intra- and interobserver reliability of quantitative PDS were estimated by intraclass correlation coefficients (ICCs). The smallest detectable change for the radiographic score change was calculated according to a previous study [10]. $P < 0.05$ indicated statistical significance. Statistical analyses were calculated with the use of Excel (Microsoft, Redmond, WA, USA) and MedCalc 12.1.4.0 (MedCalc Software, Mariakerke, Belgium).

Results

Clinical disease activity

At baseline there were no significant differences of DAS28-ESR and SDAI between the ADA and TCZ groups (Table 1). In both groups these parameters were significantly decreased from baseline to week 8, followed by sustained low disease activity (ADA: $P = 0.0007$, $P = 0.0005$; TCZ: $P < 0.0001$, $P < 0.0001$, respectively) (Table 1).

Radiographic evaluation of joint damage

At baseline there were no significant differences in total GSS (TGSS) between the ADA and TCZ groups (Table 1). In both groups the TGSS increased significantly from baseline to week 50 ($P = 0.0122$, $P = 0.0181$, respectively).

Local GSS (LGSS) was evaluated in each finger joint. In the ADA group the median of the LGSS at baseline for MCP and PIP joints was 2 [interquartile range (IQR) 2–4] and 3 (IQR 1.5–4), respectively, and in the TCZ group the median of the LGSS at baseline for MCP and PIP joints was 3 (IQR 2–4) and 3 (IQR 2–4), respectively. The smallest detectable change values was calculated for the LGSS for single MCP and PIP joints [0.33, 0.31 less than the smallest unit of GSS scoring (0.5)].

TABLE 1 Clinical and laboratory characteristics of patients at baseline

	ADA	TCZ	*P*-value
Age, mean (range), years	53 (24–78)	56.4 (33–77)	0.516
Sex, female/male, *n*	12/1	18/1	
Duration of symptoms, median (IQR), months	62 (11–147)	142 (72–178)	0.156
ESR, median (IQR), mm/h	48 (34–54)	54 (34–64)	0.389
CRP, median (IQR), mg/dl	0.51 (0.09–0.89)	1.31 (0.24–3.03)	0.089
Swollen joint count, median (IQR)	3 (2–5)	5 (3–7)	0.179
Tender joint count, median (IQR)	5 (1–8)	4 (2–9)	0.984
Patient's global assessment by VAS, median (IQR)	50 (42–65)	67 (40–80)	0.544
Examiner's global assessment by VAS, median (IQR)	40 (40–50)	50 (33–70)	0.56
DAS28-ESR (S.D.)			
Baseline	5.03 (1.16)	5.28 (1.08)	0.575
Week 8	2.96 (0.86)	2.93 (0.81)	0.936
SDAI (S.D.)			
Baseline	21 (10.5)	24.7 (11.3)	0.275
Week 8	7.61 (5.48)	8.84 (4.31)	0.60
TGSS, median (IQR)			
Baseline	99.5 (73–116)	122.75 (98.75–160.75)	0.238
Week 50	108.5 (73–134.5)	125 (99.88–164.88)	0.271

Relationship between positive synovial vascularity and radiographic progression in finger joints

In the ADA group the mean and median of local synovial vascularity at baseline for the MCP and PIP joints were 197 and 0 (range 0–3053) and 218 and 0 (range 0–2414), respectively. In the TCZ group the mean and median of local synovial vascularity at baseline for the MCP and PIP joints were 416 and 0 (range 0–4686) and 167 and 0 (range 0–3195), respectively. Local synovial vascularity in both the ADA and TCZ groups decreased significantly from baseline to week 8 (ADA: MCP $P = 0.0001$, PIP $P < 0.0001$; TCZ: MCP $P = 0.0002$, PIP $P = 0.004$). We next categorized finger joints into four groups according to the occurrence of patterns of positive synovial vascularity: joints without synovial vascularity throughout the observational period [the negative (N) group], joints with positive synovial vascularity limited to the period from the baseline to week 8 [the therapeutic response (R) group], joints with intermittent occurrence of positive synovial vascularity in the observational period [the intermittently positive (IP) group] and joints with persistent positive synovial vascularity throughout the observational period [the persistently positive (PP) group]. Each patient had a different pattern of joints with positive synovial vascularity: patients in the N group (ADA $n = 2$, TCZ $n = 2$), patients in the R group (ADA $n = 3$, TCZ $n = 3$), patients in the IP or PP groups (ADA $n = 3$, TCZ $n = 6$) and patients in the mixed R and IP or PP groups (ADA $n = 5$, TCZ $n = 7$).

The change in the LGSS (ΔLGSS) of the R group showed no progression as compared with the N group or showed improvement of joint damage in the PIP joints of the ADA treatment group (Fig. 1). We next focused on the joints with positive synovial vascularity after week 8, comprising the IP and PP groups. These joints showed an increased ΔLGSS as compared with the N group (Fig. 1). The ΔLGSS between the IP and PP groups showed no significant difference with either ADA or TCZ treatment (Fig. 1).

To analyse the relationship between synovial vascularity and ΔLGSS in more detail in the joints comprising the IP and PP groups, we calculated the sum of synovial vascularity of each finger joint from baseline to week 40 to represent the total exposure to inflammation during the treatment period. The medians of the sum of synovial vascularity with ADA therapy for the MCP and PIP joints were 1456 (range 71–6352) and 1136 (range 71–4757), respectively. The medians of the sum of synovial vascularity with TCZ therapy for the MCP and PIP joints were 2947 (range 71–11289) and 1385 (range 71–5964), respectively. We categorized these joints into two groups: those with a sum of synovial vascularity $\leqslant$ median value [the low-level (L) group], and those with a sum of synovial vascularity $>$ median value [the high-level (H) group]. There were no significant differences in the ΔLGSS between the L group and H group with either ADA or TCZ treatment (Fig. 1).

Intra- and interobserver reliability for power Doppler ultrasonography

Representative PDS images for 20 MCP and 20 PIP joints were randomly chosen, and synovial vascularity was measured three times each by the three ultrasonographers (M.H., F.S. and A.N.). The obtained intraobserver ICC values were 0.997–0.999 for MCP joints and 0.998–0.999 for PIP joints. The interobserver ICC values were 0.992–0.996 for MCP joints and 0.991–0.999 for PIP joints.

Discussion

Our study revealed two noteworthy results. First, this study further emphasized a previous report [7] that early improvement and then disappearance of synovial vascularity resulted in reducing joint damage progression.

FIG. 1 Relationship between positive synovial vascularity and LGSS in finger joints.

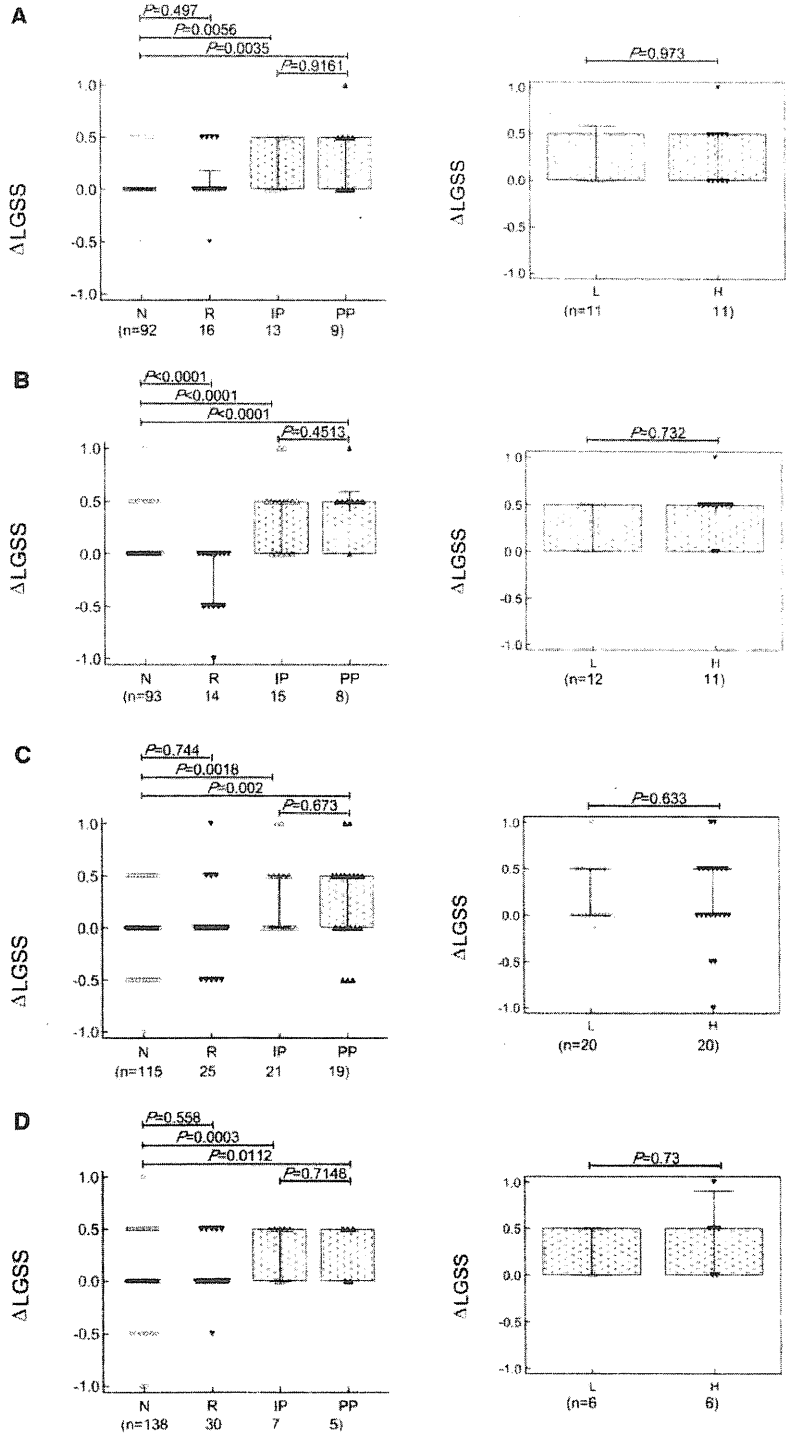

For ADA treatment, ΔLGSS of MCP (**A**) and PIP joints (**B**) is shown. For TCZ treatment, ΔLGSS of MCP (**C**) and PIP joints (**D**) is shown. Graphs on the left side show ΔLGSS of the N, R, IP and PP groups (Results section), which were categorized according to the occasional occurrence of positive synovial vascularity. For each joint in the IP and PP groups, the sum of synovial vascularity from baseline to week 40 was calculated and then categorized as L and H groups (Results section). Graphs on the right side show ΔLGSS of the L and H groups.

Secondly, a novel result was that persistence of positive synovial vascularity in local finger joints showed joint damage progression despite achieving low disease activity by biologic therapies. Interestingly, the ΔLGSS progressed independently of time-integrated joint inflammation estimated by the sum of synovial vascularity or occasional occurrence of positive synovial vascularity. These joints indicate the presence of low-level local joint inflammation, i.e. smouldering inflammation. The smouldering inflammatory joints could be categorized as a variation of subclinical synovitis described below.

Analysis of RA in the clinical remission phase revealed that there were asymptomatic or symptom-limited joints with poor prognosis. This joint inflammation or so-called subclinical synovitis can only be detected with imaging techniques [11–14]. The growing importance of imaging remission of rheumatoid activity has been confirmed, and imaging techniques such as joint ultrasonography have focused on detailed detection of local joint inflammation [15, 16].

Synovial vascularity detected by PDS is irrefutably linked to the level of joint inflammation [17, 18]. Naredo *et al.* [19] reported the correlation between time-integrated values of joint counts for positive synovial vascularity and total joint damage progression at 1 year. From these results, we speculated that increasing and persistent synovial vascularity might result in advanced joint damage progression; hence an increase in the occasional occurrence of positive synovial vascularity or the sum of synovial vascularity worsens the structural damage in smouldering inflammatory joints. Our data revealed that joints with positive synovial vascularity after week 8 (IP and PP groups) showed joint damage progression: however, their ΔLGSS progression did not relate to the occasional occurrence of positive synovial vascularity or the sum of synovial vascularity (Fig. 1). Accordingly, we concluded that the structural damage in joints with smouldering inflammation progressed independently of the level of the sum of synovial vascularity or the occasional occurrence of positive synovial vascularity. Importantly, the result might indicate that even low levels of positive synovial vascularity that occurred only once during the clinical improvement phase showed a risk for structural damage.

Although a correlation between the progression of systemic joint damage and time-integrated values of joint counts for positive synovial vascularity was reported [19], our study, which focused on synovitis and joint damage in individual finger joints, did not show such correlation. Whereas the previous study [19] showed the effect of non-biologic DMARDs, we studied biologic agents that rapidly improved acute inflammation. The DMARDs have slow therapeutic effect; thus the relationship between exposure to inflammation and joint damage progression may be closer in non-biologic DMARD users. Further, our data showed that some patients were in the mixed R and IP or PP group after starting biologic agents. This might indicate a discrepancy between overall therapeutic response and local joint response. Limitations of our study were its small scale and short observation period. Further larger studies are needed to confirm our observations.

In RA, tight control of joint inflammation is necessary for better outcomes. Treatment strategies should be changed according to the clinical response. Monitoring of synovial vascularity has the potential to provide useful joint information for daily practice and to tailor treatment strategies in RA.

Rheumatology key messages

- Finger joints with positive synovial vascularity under low disease activity showed structural deterioration in RA.
- Monitoring of synovial vascularity has the potential to provide useful information for daily practice in RA.

Disclosure statement: The authors have declared no conflicts of interest.

References

1 Jousse-Joulin S, d'Agostino MA, Marhadour T *et al.* Reproducibility of joint swelling assessment by sonography in patients with long-lasting rheumatoid arthritis (SEA-Repro study part II). J Rheumatol 2010;37:938–45.

2 Felson DT, Anderson JJ, Boers M *et al.* Preliminary definition of improvement in rheumatoid arthritis. Arthritis Rheum 1995;38:727–35.

3 Prevoo ML, van 't Hof MA, Kuper HH, van Leeuwen MA, van de Putte LB, van Riel PL. Modified disease activity scores that include twenty-eight-joint counts. Development and validation in a prospective longitudinal study of patients with rheumatoid arthritis. Arthritis Rheum 1995;38:44–8.

4 Koch AE. Review: angiogenesis: implications for rheumatoid arthritis. Arthritis Rheum 1998;41:951–62.

5 Newman JS, Adler RS, Bude RO, Rubin JM. Detection of soft-tissue hyperemia: value of power Doppler sonography. AJR Am J Roentgenol 1994;163:385–9.

6 Naredo E, Moller I, Cruz A, Carmona L, Garrido J. Power Doppler ultrasonographic monitoring of response to anti-tumor necrosis factor therapy in patients with rheumatoid arthritis. Arthritis Rheum 2008;58:2248–56.

7 Fukae J, Isobe M, Kitano A *et al.* Radiographic prognosis of finger joint damage predicted by early alteration in synovial vascularity in patients with rheumatoid arthritis: potential utility of power Doppler sonography in clinical practice. Arthritis Care Res 2011;63:1247–53.

8 Fukae J, Kon Y, Henmi M *et al.* Change of synovial vascularity in a single finger joint assessed by power Doppler sonography correlated with radiographic change in rheumatoid arthritis: comparative study of a novel quantitative score with a semiquantitative score. Arthritis Care Res 2010;62:657–63.

9 Genant HK, Jiang Y, Peterfy C, Lu Y, Redei J, Countryman PJ. Assessment of rheumatoid arthritis using

a modified scoring method on digitized and original radiographs. Arthritis Rheum 1998;41:1583–90.

10 Bruynesteyn K, Boers M, Kostense P, van der Linden S, van der Heijde D. Deciding on progression of joint damage in paired films of individual patients: smallest detectable difference or change. Ann Rheum Dis 2005;64:179–82.

11 Peluso G, Michelutti A, Bosello S, Gremese E, Tolusso B, Ferraccioli G. Clinical and ultrasonographic remission determines different chances of relapse in early and long standing rheumatoid arthritis. Ann Rheum Dis 2011;70:172–5.

12 Brown AK, Quinn MA, Karim Z *et al.* Presence of significant synovitis in rheumatoid arthritis patients with disease-modifying antirheumatic drug-induced clinical remission: evidence from an imaging study may explain structural progression. Arthritis Rheum 2006;54:3761–73.

13 Filippucci E, Iagnocco A, Meenagh G *et al.* Ultrasound imaging for the rheumatologist VII. Ultrasound imaging in rheumatoid arthritis. Clin Exp Rheumatol 2007;25:5–10.

14 Brown AK, Conaghan PG, Karim Z *et al.* An explanation for the apparent dissociation between clinical remission and continued structural deterioration in rheumatoid arthritis. Arthritis Rheum 2008;58:2958–67.

15 Saleem B, Brown AK, Keen H *et al.* Should imaging be a component of rheumatoid arthritis remission criteria? A comparison between traditional and modified composite remission scores and imaging assessments. Ann Rheum Dis 2011;70:792–8.

16 Dougados M, Devauchelle-Pensec V, Ferlet JF *et al.* The ability of synovitis to predict structural damage in rheumatoid arthritis: a comparative study between clinical examination and ultrasound. Ann Rheum Dis 2012. Advance Access published on 7 June 2012, doi:10.1136/annrheumdis-2012-201469.

17 Schirmer M, Duftner C, Schmidt WA, Dejaco C. Ultrasonography in inflammatory rheumatic disease: an overview. Nat Rev Rheumatol 2011;7:479–88.

18 Lainer-Carr D, Brahn E. Angiogenesis inhibition as a therapeutic approach for inflammatory synovitis. Nat Clin Pract Rheumatol 2007;3:434–42.

19 Naredo E, Collado P, Cruz A *et al.* Longitudinal power Doppler ultrasonographic assessment of joint inflammatory activity in early rheumatoid arthritis: predictive value in disease activity and radiologic progression. Arthritis Rheum 2007;57:116–24.

ARTHRITIS & RHEUMATISM
Vol. 64, No. 1, January 2012, pp 162–172
DOI 10.1002/art.33335

Overexpression of T-bet Gene Regulates Murine Autoimmune Arthritis

Yuya Kondo,[1] Mana Iizuka,[1] Ei Wakamatsu,[2] Zhaojin Yao,[1] Masahiro Tahara,[1] Hiroto Tsuboi,[1] Makoto Sugihara,[1] Taichi Hayashi,[1] Keigyou Yoh,[1] Satoru Takahashi,[1] Isao Matsumoto,[1] and Takayuki Sumida[1]

Objective. **To clarify the role of T-bet in the pathogenesis of collagen-induced arthritis (CIA).**

Methods. **T-bet–transgenic (Tg) mice under the control of the CD2 promoter were generated. CIA was induced in T-bet–Tg mice and wild-type C57BL/6 (B6) mice. Levels of type II collagen (CII)–reactive T-bet and retinoic acid receptor–related orphan nuclear receptor γt (RORγt) messenger RNA expression were analyzed by real-time polymerase chain reaction. Criss-cross experiments using CD4+ T cells from B6 and T-bet–Tg mice, as well as CD11c+ splenic dendritic cells (DCs) from B6 and T-bet–Tg mice with CII were performed, and interleukin-17 (IL-17) and interferon-γ (IFNγ) in the supernatants were measured by enzyme-linked immunosorbent assay. CD4+ T cells from B6, T-bet–Tg, or T-bet–Tg/IFNγ$^{-/-}$ mice were cultured for Th17 cell differentiation, then the proportions of cells producing IFNγ and IL-17 were analyzed by fluorescence-activated cell sorting.**

Results. **Unlike the B6 mice, the T-bet–Tg mice did not develop CIA. T-bet–Tg mice showed overexpression of *Tbx21* and down-regulation of *Rorc* in CII-reactive T cells. Criss-cross experiments with CD4+ T cells and splenic DCs showed a significant reduction in IL-17 production by CII-reactive CD4+ T cells in T-bet–Tg mice, even upon coculture with DCs from B6 mice, indicating dysfunction of IL-17–producing CD4+ T cells. Inhibition of Th17 cell differentiation under an in vitro condition favoring Th17 cell differentiation was observed in both T-bet–Tg mice and T-bet–Tg/IFNγ$^{-/-}$ mice.**

Conclusion. **Overexpression of T-bet in T cells suppressed the development of autoimmune arthritis. The regulatory mechanism of arthritis might involve dysfunction of CII-reactive Th17 cell differentiation by overexpression of T-bet via IFNγ-independent pathways.**

Rheumatoid arthritis (RA) is a chronic inflammatory disorder characterized by autoimmunity, infiltration of the joint synovium by activated inflammatory cells, and progressive destruction of cartilage and bone. Although the exact cause of RA is not clear, T cells seem to play a crucial role in the initiation and perpetuation of the chronic inflammation in RA.

The Th1 cell subset has long been considered to play a predominant role in inflammatory arthritis, because T cell clones from RA synovium were found to produce large amounts of interferon-γ (IFNγ) (1). Recently, interleukin-17 (IL-17)–producing Th17 cells have been identified, and this newly discovered T cell population appears to play a critical role in the development of various forms of autoimmune arthritis in experimental animals, such as those with glucose-6-phosphate isomerase–induced arthritis (2) and collagen-induced arthritis (CIA) (3). Conversely, IFNγ has antiinflammatory effects on the development of experimental arthritis (4,5). IL-17 is spontaneously produced by RA synovium (6), and the percentage of IL-17–positive CD4+ T cells

Supported in part by the Japanese Ministry of Science and Culture and by the Japanese Ministry of Health, Labor, and Welfare.

[1]Yuya Kondo, MD, Mana Iizuka, MSc, Zhaojin Yao, MSc, Masahiro Tahara, BSc, Hiroto Tsuboi, MD, PhD, Makoto Sugihara, MD, PhD, Taichi Hayashi, MD, PhD, Keigyou Yoh, MD, PhD, Satoru Takahashi, MD, PhD, Isao Matsumoto, MD, PhD, Takayuki Sumida, MD, PhD: Graduate School of Comprehensive Human Sciences, University of Tsukuba, Tsukuba City, Ibaraki, Japan; [2]Ei Wakamatsu, PhD: Graduate School of Comprehensive Human Sciences, University of Tsukuba, Tsukuba City, Ibaraki, Japan, and Harvard Medical School, Boston, Massachusetts.

Address correspondence to Takayuki Sumida, MD, PhD, Division of Clinical Immunology, Doctoral Programs in Clinical Sciences, Graduate School of Comprehensive Human Science, University of Tsukuba, 1-1-1 Tennodai, Tsukuba City, Ibaraki 305-8575, Japan. E-mail: tsumida@md.tsukuba.ac.jp.

Submitted for publication January 4, 2011; accepted in revised form September 1, 2011.

was increased in the peripheral blood mononuclear cells of patients with RA compared with healthy control subjects (7). It is therefore necessary to determine if autoimmune arthritis is a Th1- or a Th17-associated disorder.

The lineage commitment of each Th cell subset from naive CD4+ T cells is dependent on the expression of specific transcription factors induced under the particular cytokine environment. Differentiation of Th1 cells is dependent on the expression of the transcription factor T-bet, which is induced by IFNγ/STAT-1 signaling pathways and directly activates the production of IFNγ (8,9). Similarly, Th17 cell differentiation in mice is dependent on the transcription factor retinoic acid receptor–related orphan nuclear receptor γt (RORγt) induced by transforming growth factor β (TGFβ) and IL-6 (10). Previous studies showed that these transcription factors negatively regulate the differentiation of other T cell subsets by direct co-interaction and/or indirect effects of cytokines produced from each T cell subset (11,12). How the predominant differentiation of CD4+ T cells affects the development of autoimmune arthritis remains unclear, however.

In the present study, CIA was induced in C57BL/6 (B6) mice and T-bet–transgenic (Tg) mice under the control of the CD2 promoter. The results showed that CIA was significantly suppressed in T-bet–Tg mice as compared with B6 mice. IL-17 production was not detected in type II collagen (CII)–reactive T cells from T-bet–Tg mice, and a significant reduction in IL-17 production by CII-reactive CD4+ T cells from T-bet–Tg mice was observed even when they were cocultured with splenic dendritic cells (DCs) from B6 mice. IFNγ production was also reduced in T-bet–Tg mice as compared with B6 mice, and levels of IFNγ in CII-reactive CD4+ T cells from T-bet–Tg mice were not different from those in B6 mice. Inhibition of Th17 cell differentiation and predominant differentiation of Th1 cells under an in vitro condition favoring Th17 cell differentiation was observed in T-bet–Tg mice, and surprisingly, this inhibition was also observed in T-bet–Tg/IFNγ$^{-/-}$ mice. These results indicate suppression of Th17 cell differentiation by overexpression of T-bet, but not IFNγ. Our findings support the notion that the suppression of autoimmune arthritis in T-bet–Tg mice might be due to the direct inhibition of Th17 cell differentiation by T-bet overexpression in T cells.

MATERIALS AND METHODS

Mice. CD2 T-bet–Tg mice (12) were prepared by backcrossing mice on a C57BL/6 background. IFNγ$^{-/-}$ mice were obtained from The Jackson Laboratory. Littermates of T-bet–Tg mice were used as controls in all experiments. All mice were maintained under specific pathogen–free conditions, and the experiments were conducted in accordance with the institutional ethics guidelines.

Induction of CIA and assessment of arthritis. Native chicken CII (Sigma-Aldrich) was dissolved in 0.01*M* acetic acid and emulsified in Freund's complete adjuvant (CFA). CFA was prepared by mixing 5 mg of heat-killed *Mycobacterium tuberculosis* H37Ra (Difco) and 1 ml of Freund's incomplete adjuvant (Sigma-Aldrich). Mice ages 8–10 weeks were injected intradermally at the base of the tail with 200 μg of CII in CFA on days 0 and 21. Arthritis was evaluated visually, and changes in each paw were scored on a scale of 0–3, where 0 = normal, 1 = slight swelling and/or erythema, 2 = pronounced swelling, and 3 = ankylosis. The scores in the 4 limbs were then summed (maximum score 12).

Histopathologic scoring. For histologic assessment, mice were killed on day 42 after the first immunization, and both rear limbs were removed. After fixation and decalcification, joint sections were cut and stained with hematoxylin and eosin. Histologic features of arthritis were quantified by 2 independent observers (YK and IM) who were blinded with regard to the study group, and a histologic score was assigned to each joint based on the degree of inflammation and erosion, as described previously (13). The severity of inflammation was scored on a scale of 0–5, where 0 = normal, 1 = minimal inflammatory infiltration, 2 = mild infiltration with no soft tissue edema or synovial lining cell hyperplasia, 3 = moderate infiltration with surrounding soft tissue edema and some synovial lining cell hyperplasia, 4 = marked infiltration, edema, and synovial lining cell hyperplasia, and 5 = severe infiltration with extended soft tissue edema and marked synovial lining cell hyperplasia. The severity of bone erosion was also scored on a scale of 0–5, where 0 = none, 1 = minimal, 2 = mild, 3 = moderate, 4 = marked, and 5 = severe erosion with full-thickness defects in the cortical bone.

Analysis of cytokine profiles and cytokine and transcriptional factor gene expression. Inguinal and popliteal lymph nodes were harvested from each mouse on day 10 after the first immunization with CII. Single-cell suspensions were prepared, and lymph node cells (2×10^5/well on a 96-well round-bottomed plate) were cultured for 72 hours in RPMI 1640 medium (Sigma-Aldrich) containing 10% fetal bovine serum, 100 units/ml of penicillin, 100 μg/ml of streptomycin, and 50 μ*M* 2-mercaptoethanol in the presence of 100 μg/ml of denatured chicken CII. The supernatants were analyzed for IFNγ, IL-4, IL-10, and IL-17 by enzyme-linked immunosorbent assay (ELISA) using specific Quantikine ELISA kits (R&D Systems).

Lymphocytes harvested on day 10 after immunization were used to obtain complementary DNA (cDNA) by reverse transcription, using a commercially available kit. A TaqMan Assay-on-Demand gene expression product was used for real-time polymerase chain reaction (PCR; Applied Biosystems). The expression levels of *Ifng*, *Il17a*, *Tbx21*, *Rorc*, *Il12a*, and *Il23a* were normalized relative to the expression of *gapdh*. Analyses were performed with an ABI Prism 7500 apparatus (Applied Biosystems).

Criss-cross coculture with CD4+ T cells and CD11c+ splenic dendritic cells. Ten days after the first CII immunization, CD4+ cells in draining lymph nodes were isolated by

positive selection, using a magnetic-activated cell sorter (MACS) system with anti-CD4 monoclonal antibody (mAb; Miltenyi Biotec). After treatment with mitomycin C, CD11c+ cells were isolated from the spleen by positive selection, using a MACS system with anti-CD11c mAb (Miltenyi Biotec). Criss-cross coculture for 72 hours was performed with 1×10^5 CD4+ cells and 2×10^4 CD11c+ cells in 100 μg/ml of denatured CII-containing medium. Cytokine production and transcription factor expression were then analyzed.

Measurement of collagen-specific immunoglobulin titers. Serum was collected from the mice on day 56 after the first immunization. A total of 10 μg/ml of CII in phosphate buffered saline (PBS) was coated overnight at 4°C onto 96-well plates (Nunc MaxiSorp; Nalge Nunc). After washes with washing buffer (0.05% Tween 20 in PBS), the blocking solution, including 1% bovine serum albumin in PBS, was applied for 1 hour. After washing, 100 μl of diluted serum was added, and the plates were incubated for 1 hour at room temperature. After further washing, horseradish peroxidase–conjugated anti-mouse IgG, IgG1, IgG2a, or IgG2b (1:5,000 dilution) in blocking solution was added, and the plates were incubated for 1 hour at room temperature. After washing, tetramethylbenzidine was added, and the optical density was read at 450 nm using a microplate reader.

Purification of CD4+ cells and in vitro T cell cultures. CD4+ cells (1×10^6/well) were cultured in medium with 1 μg/ml of soluble anti-CD3ε mAb (eBioscience), 1 μg/ml of soluble anti-CD28 mAb (BioLegend), 10 μg/ml of anti-IFNγ mAb (BioLegend), and 10 μg/ml of anti–IL-4 mAb (BioLegend) for a neutral condition. For Th17 cell differentiation, CD4+ cells (1×10^6/well) were cultured in medium with 1 μg/ml of soluble anti-CD3ε mAb, 1 μg/ml of soluble anti-CD28 mAb, 3 ng/ml of human TGFβ (R&D Systems), 20 ng/ml of mouse IL-6 (eBioscience), 10 μg/ml of anti-IFNγ mAb, and 10 μg/ml of anti–IL-4 mAb. On day 4, cells were restimulated for 4 hours with 50 ng/ml of phorbol myristate acetate and 500 ng/ml of ionomycin and used in the experiments.

Surface and intracellular staining and fluorescence-activated cell sorter (FACS) analysis. GolgiStop (BD PharMingen) was added during the last 6 hours of each culture. Cells were stained extracellularly, fixed, and permeabilized with Cytofix/Cytoperm solution (BD PharMingen). Then, intracellular cytokine staining was performed according to the manufacturer's protocol, using fluorescein isothiocyanate (FITC)–conjugated anti-IFNγ (BD PharMingen) and phycoerythrin (PE)–conjugated anti–IL-17 (BD PharMingen) or FITC-conjugated anti–IL-17 (BioLegend). A Treg cell staining kit (eBioscience) was used to stain T-bet, RORγt, and FoxP3 in cultured cells according to the manufacturer's protocol, using PE-conjugated anti–T-bet (eBioscience), allophycocyanin-conjugated anti-RORγt (eBioscience), and PE-conjugated anti-FoxP3 (eBioscience). Samples were analyzed with a FACSCalibur flow cytometer (Becton Dickinson), and data were analyzed with FlowJo software (Tree Star).

Statistical analysis. Data are expressed as the mean ± SEM or the mean ± SD. Differences between groups were examined for statistical significance using Student's *t*-test. *P* values less than 0.05 were considered significant.

RESULTS

Construction of the T-bet transgene and tissue distribution of transcription factors and cytokine production in naive mice. To generate transgenic mouse lines that express high levels of T-bet specifically in T cells, mouse T-bet cDNA was inserted into a VA vector containing a human CD2 transgene cassette (14). To confirm the expression of the transgene, reverse transcription–PCR (RT-PCR) was performed to monitor the expression of *Tbx21* (coding for T-bet) in organs from the T-bet–Tg mice. *Tbx21* messenger RNA (mRNA) expression was detected in the lymphatic system and in nonlymphatic organs in T-bet–Tg mice, and the expression levels were higher than those in B6 mice (data available upon request from the author). Analysis by semiquantitative RT-PCR and quantitative PCR (data not shown) revealed that the expression levels of other transcription factors (*Gata3*, *Rorc*, and *Foxp3*) in T-bet–Tg mice were not different from those in B6 mice. As previously reported by Ishizaki et al (14), high production of IFNγ was observed even when CD4+ T cells isolated from the spleen of T-bet–Tg mice were cultured under neutral conditions (data available upon request from the author).

Failure to induce CIA and low CII-specific IgG production in T-bet–Tg mice. To assess whether T cell–specific T-bet expression affects the development of arthritis, we induced CIA in T-bet–Tg mice and in wild-type B6 mice. The incidence and severity of arthritis in T-bet–Tg mice were markedly suppressed compared with those in B6 mice (Figure 1A). Surprisingly, the majority of T-bet–Tg mice were essentially free of arthritis, and even when arthritis was present, it was of the mild type. Consistent with these findings, histologic analyses of the joints obtained from each mouse 42 days after immunization revealed that joint inflammation and destruction were significantly suppressed in T-bet–Tg mice compared with B6 mice (Figures 1B and C). These results indicated that enforced expression of T-bet in T cells suppressed the development of CIA.

Because the levels of CII-specific IgG correlate well with the development of arthritis (15), we examined CII-specific IgG production in T-bet–Tg mice. CII-specific IgG, IgG1, IgG2a, and IgG2b levels were significantly lower in T-bet–Tg mice than in B6 mice, as determined by ELISA (Figure 1D). Thus, enforced expression of T-bet in T cells suppresses the development of CIA and CII-specific IgG production.

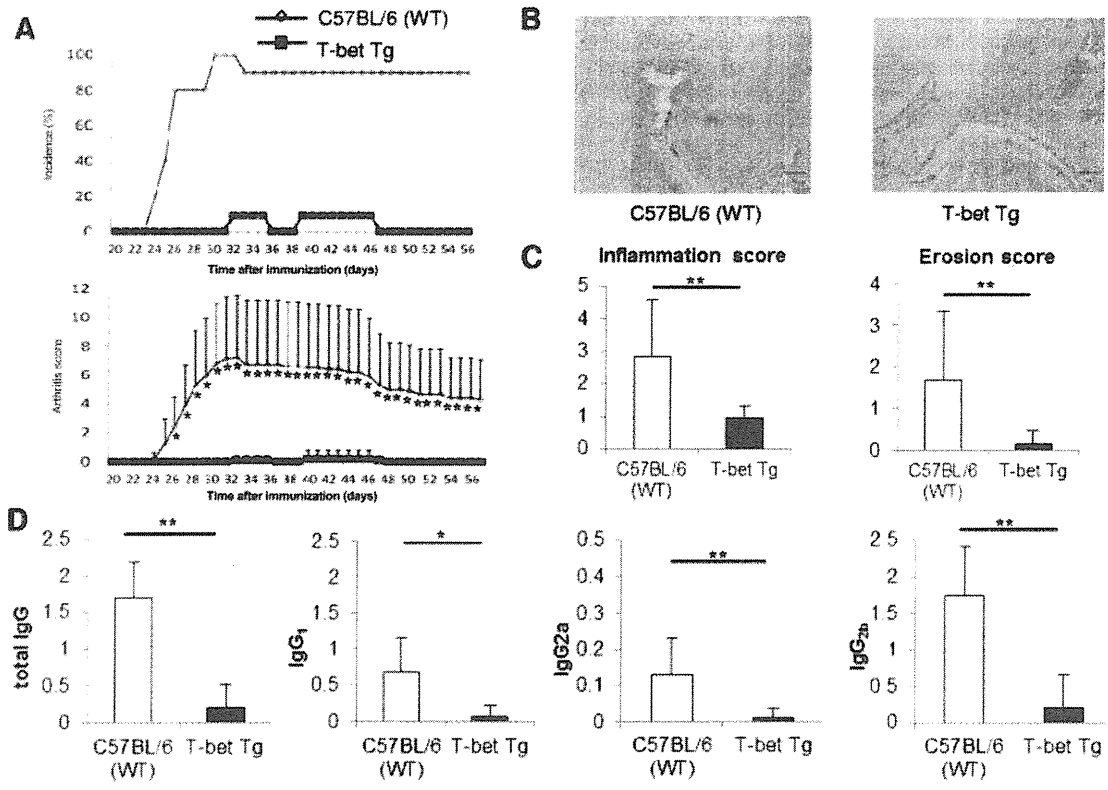

Figure 1. Significant suppression of collagen-induced arthritis (CIA) and type II collagen (CII)–specific IgG production in T-bet–transgenic (Tg) mice. On days 0 and 21, mice were immunized intradermally at several sites at the base of the tail with chicken CII emulsified with Freund's complete adjuvant. **A,** Incidence and severity of CIA. The arthritis score was determined as described in Materials and Methods. Data were obtained from 2 independent experiments involving 10 C57BL/6 (wild-type [WT]) mice and 11 T-bet–Tg mice. **B,** Hematoxylin and eosin–stained sections of the hind paws of mice obtained 6 weeks after the first immunization. Original magnification × 40. **C,** Inflammation and bone erosion scores in 7 C57BL/6 mice and 5 T-bet–Tg mice 6 weeks after the first immunization. Scores were determined as described in Materials and Methods. **D,** Serum levels of CII-specific IgG, IgG1, IgG2a, and IgG2b levels in 10 C57BL/6 mice and 11 T-bet–Tg mice 8 weeks after the first immunization, as measured by enzyme-linked immunosorbent assay. Values in **A, C,** and **D** are the mean ± SD. * = $P < 0.05$; ** = $P < 0.01$ by Student's *t*-test.

Suppression of CII-reactive IL-17 production and IL-17 mRNA expression in T-bet–Tg mice. Because enforced T-bet expression in T cells suppressed the development CIA, we examined antigen-specific cytokine production and transcription factor expression in mice with CIA. CD4+ T cells harvested from draining lymph nodes were stimulated with CII in vitro, and then various cytokine levels in the supernatants were measured by ELISA. IL-17 production by CII-reactive T cells was significantly reduced in T-bet–Tg mice as compared with B6 mice (Figure 2A). IFNγ production by CII-reactive T cells also tended to be decreased in T-bet–Tg mice.

We analyzed CII-reactive cytokine and transcription factor mRNA expression levels by real-time PCR (Figure 2B). Similar to the ELISA results, *Il17a* expression tended to be lower in T-bet–Tg mice than in B6 mice. No difference in *Ifng* expression was observed between B6 and T-bet–Tg mice (Figure 2B). *Tbx21* expression tended to be higher in T-bet–Tg mice, whereas *Rorc* expression was lower in T-bet–Tg mice than in B6 mice ($P < 0.05$). The level of expression of *Il12a* (coding for IL-12p35) was also higher in T-bet–Tg mice than in B6 mice ($P < 0.05$). However, there was no difference in the expression levels of *Il23a* (coding for IL-23p19) between B6 mice and T-bet–Tg mice. These

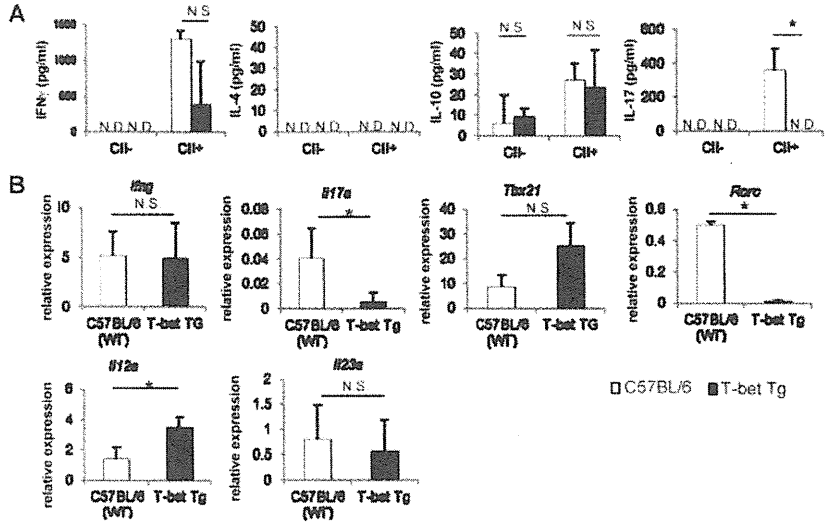

Figure 2. No production of interleukin-17 (IL-17) and low production of interferon-γ (IFNγ) in type II collagen (CII)–reactive CD4+ T cells. **A,** Ten days after the first CII immunization, lymphocytes derived from the draining lymph nodes of C57BL/6 (wild-type [WT]) mice and T-bet–transgenic (Tg) mice were cultured for 72 hours in the presence or absence of 100 μg/ml of denatured CII. Levels of IL-17, IFNγ, IL-4, and IL-10 in the supernatants were measured by enzyme-linked immunosorbent assay. **B,** After culture of lymphocytes with CII, cDNA was obtained, and levels of *Ifng*, *Il17a*, *Tbx21*, *Rorc*, *Il12a*, and *Il23a* expression were analyzed by real-time polymerase chain reaction. Values are the mean ± SD of 3 mice. * = $P < 0.05$ by Student's *t*-test. ND = not detected; NS = not significant.

results suggest that overexpression of T-bet on CD4+ T cells suppressed the expression of RORγt and IL-17.

No reduction of RORγt expression on CII-reactive CD4+ T cells in T-bet–Tg mice. CD4+ T cells from T-bet–Tg and B6 mice were cultured in vitro with CII, and analyses of T-bet and RORγt expression on CD4+ T cells were carried out by the intracellular staining method. T-bet expression on CII-reactive CD4+ T cells was significantly higher in T-bet–Tg mice than in B6 mice (Figure 3A). Surprisingly, the majority of T-bet+ CII-reactive T cells expressed RORγt in both the B6 mice and the T-bet–Tg mice (Figure 3A). Although there was no significant difference in the mean fluorescence intensity of RORγt between B6 mice and T-bet–Tg mice, the number of RORγt+ cells tended to be lower in T-bet–Tg mice (data available upon request from the author).

Moreover, in the case of CD4+ T cells examined under conditions favoring Th17 differentiation, RORγt expression on CD4+ T cells from T-bet–Tg mice was lower than that on cells from B6 mice (Figure 3B). Interestingly, most of the RORγt+ cells also expressed T-bet in the T-bet–Tg mice, and the proportion of IL-17–producing RORγt+ CD4+ T cells was lower in the T-bet–Tg mice than in the B6 mice. These findings support the notion that overexpression of T-bet not only suppresses RORγt expression on CD4+ T cells but also inhibits the production of IL-17 from RORγt+ T cells.

To investigate whether the suppression of arthritis and low antigen-specific cytokine production observed in T-bet–Tg mice was related to Treg cells, the next experiment analyzed FoxP3 expression on CD4+ T cells harvested from draining lymph nodes 10 days after immunization. There was no significant difference in the percentage of FoxP3+ cells among the CD4+ T cells between B6 mice and T-bet–Tg mice (data available upon request from the author). Thus, Treg cells do not seem to be involved in the suppression of CIA in T-bet–Tg mice.

Decreased numbers of T cells in the lymph nodes, spleen, and thymus of T-bet–Tg mice. To evaluate the low cytokine response and the low population of CII-reactive RORγt+CD4+ T cells in T-bet–Tg mice with CIA, we analyzed the lymphocyte subsets in the draining lymph nodes and spleen after immunization. The percentage and absolute number of CD3+ T cells were lower in both the draining lymph nodes and the

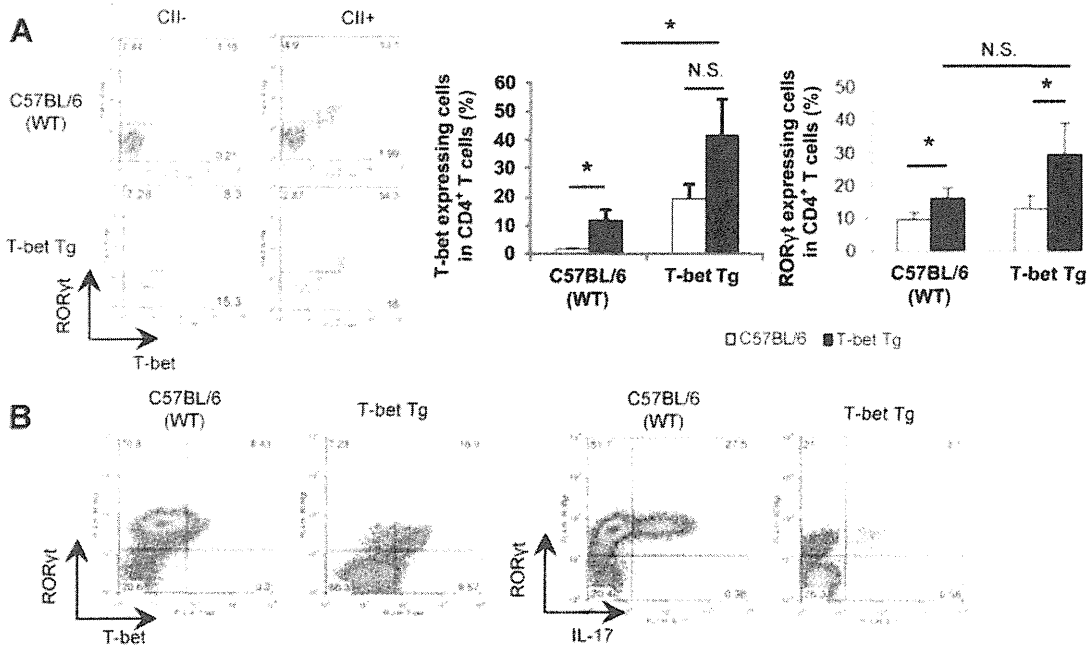

Figure 3. Suppression of Th17 cell differentiation by enforced expression of T-bet in T cells despite expression of retinoic acid receptor–related orphan nuclear receptor γt (RORγt). **A,** Ten days after the first type II collagen (CII) immunization, lymphocytes derived from the draining lymph nodes of C57BL/6 (wild-type [WT]) and T-bet–transgenic (Tg) mice were cultured for 72 hours in the presence or absence of 100 μg/ml of denatured CII. Levels of T-bet and RORγt expression on CD4+ T cells were analyzed by intracellular staining. Numbers in each compartment of the histograms are the percentage of transcription factor–expressing cells gated on CD4+ T cells. Values in the bar graphs are the mean ± SD of 3 mice per group. * = $P < 0.05$ by Student's t-test. NS = not significant. **B,** CD4+ T cells were isolated from the spleen of C57BL/6 and T-bet–Tg mice by magnetic-activated cell sorting and were then cultured for 96 hours with soluble anti-CD3 antibody, soluble anti-CD28 antibody, interleukin-6 (IL-6), and transforming growth factor β. Cytokine production and transcription factor expression on CD4+ T cells were analyzed by intracellular staining. Representative histograms from flow cytometric analysis of T-bet and RORγt expression with IL-17 production are shown. Numbers in each compartment are the percentage of positive cells gated on CD4+ T cells.

spleen of T-bet–Tg mice as compared with B6 mice (Figures 4A and B). The absolute number of CD4+ and CD8+ T cells also tended to be lower in T-bet–Tg mice (Figure 4B). Moreover, analysis of the thymus showed a significantly low number of total thymocytes in T-bet–Tg mice and the presence of an abnormal proportion of T precursor cells, such as a low number of double-positive T cells and CD4 single-positive T cells in T-bet–Tg mice (Figure 4C). These results suggest abnormal T cell development in the thymus of T-bet–Tg mice.

Inhibition of IL-17 production by CII-reactive CD4+ T cells in T-bet–Tg mice. To clarify whether T-bet overexpression on CD4+ T cells directly affects cytokine production, we performed criss-cross experiments using CD4+ T cells from B6 and T-bet–Tg mice, as well as DCs from B6 and T-bet–Tg mice in CII–containing medium, and measured IL-17 and IFNγ levels in the supernatants by ELISA. IL-17 production was detected in CII-reactive CD4+ T cells from B6 mice and in DCs from T-bet–Tg mice. Interestingly, IL-17 production was significantly reduced, even when CD4+ T cells from T-bet–Tg mice were cocultured with DCs from B6 mice (Figure 5A). These observations suggest that T-bet overexpression on CD4+ T cells is responsible for the inhibition of CII-reactive IL-17 production. No difference in IFNγ production was noted among the experimental conditions (Figure 5A), suggesting that reduced IFNγ production by CII-reactive CD4+ T cells from T-bet–Tg mice (Figure 2) was probably related to the reduced numbers of CD4+ T cells in draining lymph nodes. Moreover, intracellular staining revealed that RORγt expression was suppressed and T-bet expression was increased, even when CD4+ T cells from T-bet–Tg

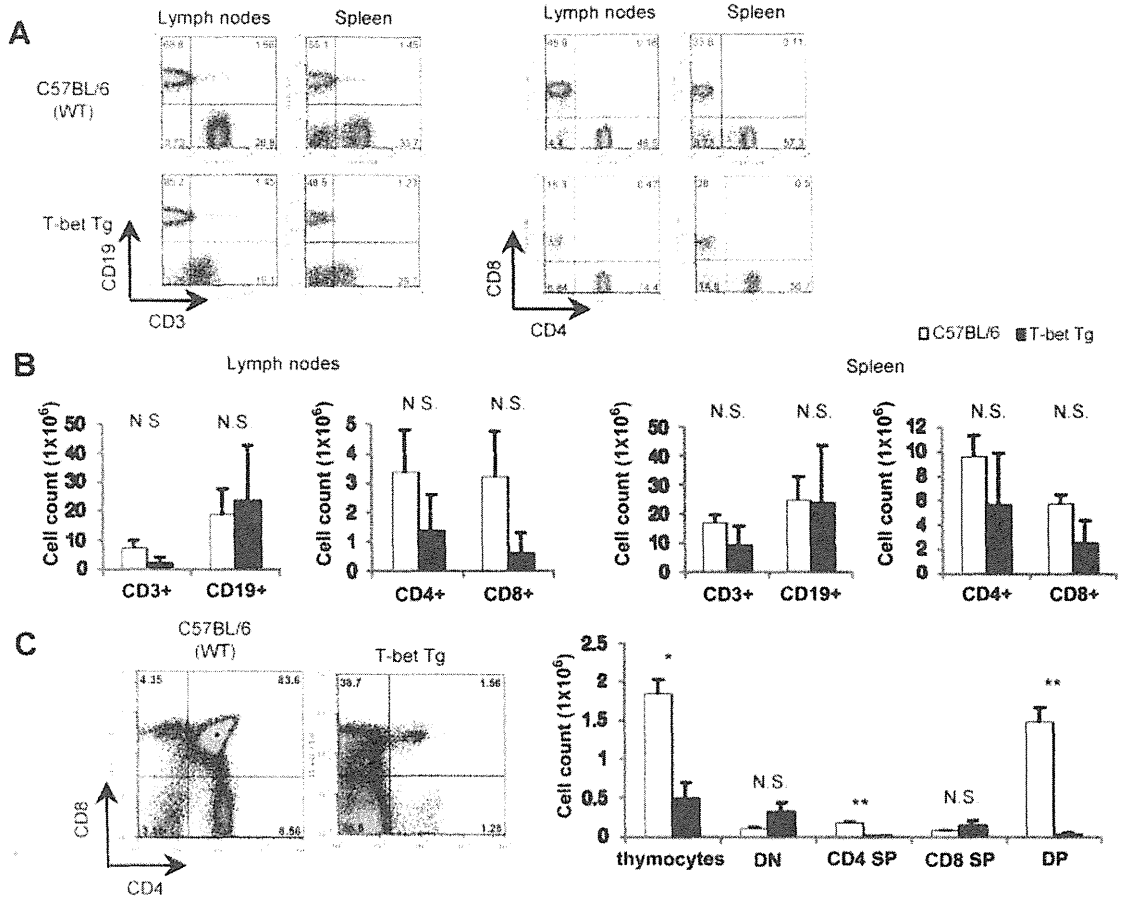

Figure 4. Decreased number of CD3+ T cells in spleen and lymph nodes and abnormal development of T precursor cells in the thymus in T-bet–transgenic (Tg) mice. **A,** Ten days after first immunization, the proportion of lymphocytes in draining lymph nodes and spleen were analyzed by fluorescence-activated cell sorting (FACS), and the absolute numbers of cells were calculated. Numbers in each compartment are the percentage of the parent population. **B,** The absolute numbers of CD3+, CD19+, CD4+, and CD8+ T cells in the lymph nodes and spleen of C57BL/6 (wild-type [WT]) and T-bet–Tg mice were determined. Values are the mean ± SD of 3 mice per group. NS = not significant. **C,** The proportion of T precursor cells in the thymus of nonimmunized mice was analyzed by FACS, and the absolute numbers of thymocytes, double-negative (DN) T cells, CD4 and CD8 single-positive (SP) T cells, and double-positive (DP) T cells were determined. Values in the bar graphs are the mean ± SD of 3 mice per group. * = $P < 0.05$; ** = $P < 0.01$ by Student's *t*-test.

mice were cocultured with DCs from B6 mice (Figure 5B). These results indicate that T-bet overexpression on CD4+ T cells suppressed CII-reactive IL-17 production by inhibition of the expression of RORγt.

Overexpression of T-bet directly suppresses Th17 cell differentiation via IFNγ-independent mechanisms. To clarify whether IFNγ production influences Th17 cell differentiation, we generated T-bet–Tg/IFNγ$^{-/-}$ mice. CD4+ T cells were isolated from the spleen of T-bet–Tg, T-bet–Tg/IFNγ$^{-/-}$, and B6 mice and were then cultured for Th17 cell differentiation. FACS analysis demonstrated that the proportion of IL-17–producing CD4+ T cells was lower in T-bet–Tg mice than in B6 mice, whereas the proportion of IFNγ-producing CD4+ T cells was higher in T-bet–Tg mice. Similarly, the proportion of IL-17–producing CD4+ T cells was also lower in T-bet–Tg/IFNγ$^{-/-}$ mice, although no IFNγ-producing CD4+ T cells were detected in